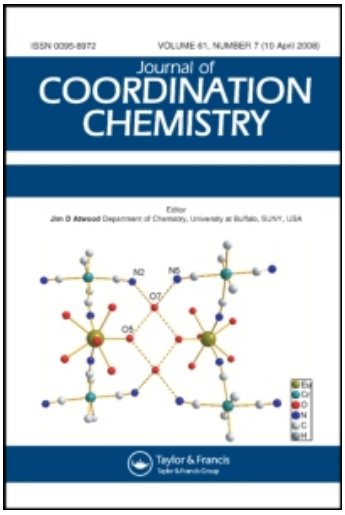

Journal of Coordination Chemistry
Publication details, including instructions for authors and subscription information:
http://www.informaworld.com/smpp/title~content=t713455674

Synthesis, crystal structure, and properties of a new 1-D "heteropoly blue"-modified nickel complex

Zhifeng Zhao[a]; Baibin Zhou[ab]; Zhanhua Su[b]
[a] School of Chemical Engineering and Technology, Harbin Institute of Technology, Harbin 150001, China [b] College of Chemistry and Chemical Engineering, Harbin Normal University, Harbin 150025, China

First published on: 24 February 2010

To cite this Article Zhao, Zhifeng , Zhou, Baibin and Su, Zhanhua(2010) 'Synthesis, crystal structure, and properties of a new 1-D "heteropoly blue"-modified nickel complex', Journal of Coordination Chemistry, 63: 5, 776 — 784, First published on: 24 February 2010 (iFirst)
To link to this Article: DOI: 10.1080/00958971003657669
URL: http://dx.doi.org/10.1080/00958971003657669

Journal of Coordination Chemistry
Vol. 63, No. 5, 10 March 2010, 776–784

Synthesis, crystal structure, and properties of a new 1-D "heteropoly blue"-modified nickel complex

ZHIFENG ZHAO†, BAIBIN ZHOU*†‡ and ZHANHUA SU‡

†School of Chemical Engineering and Technology, Harbin Institute of Technology, Harbin 150001, China
‡College of Chemistry and Chemical Engineering, Harbin Normal University, Harbin 150025, China

(*Received 14 June 2009; in final form 29 October 2009*)

A new reduced molybdenum phosphate, $[Ni(bpy)_2(H_2O)_2]\{[Ni(H_2O)_2][Ni_{0.5}(MoO_2)_6(OH)_3(PO_4)(HPO_4)_3[Ni(bpy)_2(H_2O)]_2][Ni_{0.5}(MoO_2)_6(OH)_3(PO_4)(H_2PO_4)_2(HPO_4)]\} \cdot 14H_2O$ (**1**) (2,2′-bpy = 2,2-bipyridine), has been hydrothermally synthesized and characterized by elemental analysis, IR, UV-Vis, TG, and single-crystal X-ray diffraction. Compound **1** crystallizes in the triclinic system, space group *P-1*, with lattice parameters $a = 17.0459(9)$ Å, $b = 19.2643(11)$ Å, $c = 19.9357(11)$ Å, $\beta = 79.9500(10)^\circ$, $V = 5804.9(6)$ Å, $Z = 2$, and $R_1(wR_2) = 0.0460(0.1228)$. Structural analysis indicates that neighboring $Ni[P_4Mo_6]_2$ and nickel-complex polyanions are interconnected by $[Ni(H_2O)_2]$ subunits *via* P–O–Ni(2) bridges, generating a 1-D infinite chain "heteropoly blue" structure. Furthermore, **1** shows photoluminescence in the solid state at room temperature. Compound **1** was used as a solid bulk modifier to fabricate a carbon paste electrode (**1**-CPE) by direct mixing. The electrochemical and electrocatalytic behaviors of **1**-CPE have been studied.

Keywords: Reduced molybdenum phosphate; Nickel complex; Photoluminescence; Electrochemical

1. Introduction

Polyoxometalates (POMs) have been studied extensively owing to their structural diversity, fascinating properties, and potential applications in catalysis, photochemical, electrochemical, material science, medicine, and magnetochemistry [1–3]. As a branch of POM solid materials, the most reported molybdenum or tungsten phosphates are based on Keggin or Dawson anions [4, 5], such as $\{[Co(dpdo)_4(H_2O)_2][H(H_2O)_6](PMo_{12}O_{40})\}_n$ and $H_2[Ca_2(P_2W_{18}O_{62})(H_2O)_5] \cdot 7.5H_2O$ [6, 7]. 'Heteropoly blues' in their reduced forms receive attention because of its capability of allowing a variety of chemical reactions to take place in the intracrystalline region [8, 9]. The $[P_4Mo_6O_{28-x}(OH)_{3+x}]^{(9-x)-}$ anion (denoted $[P_4Mo_6]$) with various degrees of protonation is a very stable structural unit and the most often encountered reduced molybdenum phosphates [10]. An important advance in the synthesis of reduced

*Corresponding author. Email: zhou_bai_bin@163.com

Journal of Coordination Chemistry
ISSN 0095-8972 print/ISSN 1029-0389 online © 2010 Taylor & Francis
DOI: 10.1080/00958971003657669

molybdenum phosphates is the introduction of secondary transition metal fragments, which can serve as bridging ligands, grafted into the backbone of 'heteropoly blues'. Introduction of transition metal fragments enriches the framework of molybdenum phosphates and also improves their chemical properties [11–13]. Other groups have synthesized the reduced molybdenum phosphates with $[P_4Mo_6]$ building units ranging from 1-D polymers [14, 15], 2-D layer structures [16, 17], and 3-D microporous solids [18, 19]. In these reports, $[P_4Mo_6]$ mostly modified by alkali metal cations or transition metal cations, with four nickel complexes covalently bonded to the framework of a $Ni[P_4Mo_6]_2$ unit forming 'butterflies' is first reported. As part of our effort in the hydrothermal assembly of new solid materials [20–22], we try to find reaction condition to obtain new material based on reduced molybdenum phosphate building units and TMCs with novel structures and interesting properties and then further investigate their applications in material science. Herein, we report the syntheses, structural characterization, and properties of a new reduced molybdenum phosphate, $[Ni(bpy)_2(H_2O)_2]\{[Ni(H_2O)_2][Ni_{0.5}(MoO_2)_6(OH)_3(PO_4)(HPO_4)_3[Ni(bpy)_2(H_2O)]_2][Ni_{0.5}(MoO_2)_6(OH)_3(PO_4)(H_2PO_4)_2(HPO_4)]\}\cdot 14H_2O$ (**1**). To the best of our knowledge, **1** represents the first example of 1-D chain 'heteropoly blue' based alternately on $Ni[P_4Mo_6]_2$ and modified nickel-complex clusters connected by $[Ni(H_2O)_2]$ subunits.

2. Experimental

2.1. *Materials and general methods*

All reagents were purchased commercially and used without purification. Elemental analyses (C, H, and N) were performed on a Perkin-Elmer 2400 CHN elemental analyzer (Perkin-Elmer, USA). The IR spectrum was obtained on an Alpha Centauri Fourier transform IR (FT-IR) spectrometer with KBr pellets from 400 to 4000 cm^{-1} (Mattson, USA). UV-Vis spectrum was recorded with a Lambda900 spectrometer (Perkin-Elmer, USA). The thermogravimetric analysis (TGA) was carried out in N_2 on a Perkin-Elmer DTA 1700 differential thermal analyzer with a rate of 10°C min^{-1} (Perkin-Elmer, USA). Excitation and emission spectra were obtained on a SPEX FL-2T2 spectrofluorometer equipped with a 450 W xenon lamp as the excitation source (SPEX, USA). Electrochemical measurements were performed with a CHI 660b electrochemical workstation (CHENHUA, China). A conventional three-electrode system was used. Ag/AgCl (3 M KCl) electrode was used as a reference electrode, and a Pt wire as a counter electrode. Compound **1**-modified carbon paste electrode (**1**-CPE) was used as the working electrode.

2.2. *Synthesis of 1*

$Na_2MoO_4\cdot 2H_2O$ (0.643 g, 2.657 mM), $Ni(CH_3COO)_2\cdot 4H_2O$ (0.247 g, 0.993 mM), 2,2′-bpy (0.196 g, 1.255 mM), H_3PO_4 (1 mL), and 14 mL H_2O were stirred for 80 min in air. The resulting gel was then transferred to a 20 mL Teflon-lined autoclave and kept at 160°C for 6 days. After the mixture was slowly cooled to room temperature, brown block crystals were isolated in 37% yield (based on Mo). Elemental analysis for **1**, Calcd (%): C, 18.03; H, 2.57; N, 4.21. Found (%): C, 17.98; H, 2.61; N, 4.19.

2.3. *X-ray crystallographic study*

A brown crystal of **1** was glued on a glass fiber. Data were collected on a Bruker SMART APEX II CCD diffractometer using Mo-Kα radiation (0.71073 Å) at 273 K from $2.36 < \theta < 28.34$. The structure was solved by direct methods and refined by the full-matrix least-squares on F^2 using the SHELXL-97 software package [23, 24]. All non-hydrogen atoms were refined anisotropically. Hydrogens on carbon and nitrogen were included at calculated positions and refined with a riding model. The crystal data and structure refinement of **1** are summarized in table 1. Selected bond lengths and angles are listed in table S1.

3. Results and discussion

3.1. *Synthesis*

In comparison to the reported reduced molybdenum phosphates [25], we find that bpy is a better reducing agent, and hence Mo^{6+} is readily reduced at higher temperature to form Mo^{5+}. The bpy used as templates in this work were employed to examine the nature of the molybdenum(V) formed. In the process of hydrothermal synthesis, many factors can affect the formation and crystal growth of products, such as the type of initial reactants, molar ratio, pH, reaction time, and temperature. In this case, the pH of the reaction system was crucial in the synthesis. We varied the pH to understand its effect on the nature of the products formed. Compound **1** was obtained only in a limited pH range (4.5–5.0), otherwise unknown powder instead of **1** would be obtained.

Table 1. Crystal data and structure refinement for **1**.

Empirical formula	$C_{60}H_{102}Mo_{12}N_{12}Ni_5O_{82}P_8$
Formula weight	3996.13
Temperature (K)	273(2)
Wavelength (Å)	0.71073
Crystal system	Triclinic
Space group	*P-1*
Units of dimensions (Å, °)	
a	17.0459(9)
b	19.2643(11)
c	19.9357(11)
α	86.9460(10)
β	79.9500(10)
γ	64.2670(10)
Volume (Å^3), *Z*	5804.9(6), 2
Absorption coefficient (Mo-Kα) (mm^{-1})	2.267
F(000)	3932
θ range for data collection (°)	2.36–28.34
Limiting indices	$-22 \le h \le 22$; $-25 \le k \le 25$; $-26 \le l \le 26$
Reflections collected	58355
Independent reflection	28149 [R(int) = 0.0190]
Goodness-of-fit on F^2	1.077
Final R indices [$I > 2\sigma(I)$]	$R_1 = 0.0460$, $wR_2 = 0.1228$
R indices (all data)	$R_1 = 0.0532$, $wR_2 = 0.1276$

$R_1 = \sum||F_o| - |F_c||/\sum|F_o|$; $wR_2 = \{Rw[(F_o)^2 - (F_c)^2]^2/Rw[(F_o)^2]^2\}^{1/2}$.

3.2. *Structure description*

The single-crystal X-ray analysis reveals that two neighboring $Ni_{0.5}[P_4Mo_6]$ clusters ($[Ni_{0.5}(Mo_6O_{15})(PO_4)(HPO_4)_3][Ni(bpy)_2(H_2O)]_2$ and $[Ni_{0.5}(Mo_6O_{15})(PO_4)(H_2PO_4)_2(HPO_4)]$) in **1** are linked *via* $[Ni(H_2O)_2]$ subunits. As shown in figure 1, the $[P_4Mo_6]$ cluster has a ring of six edge-sharing MoO_6 octahedra with alternating three long Mo···Mo contacts (avg. 3.519 Å) and three short Mo–Mo single bonds (avg. 2.599 Å). A central phosphate bridges the ring internally and each one of the other three phosphate groups bridges one long Mo···Mo contact externally. The P–O bond length is in the range 1.488(4)–1.602(4) Å.

There are six crystallographically independent Ni atoms in **1**: the octahedrally coordinated Ni1 and Ni5 are capped and coordinated with six oxygens (O5, O11, O21, O5A, O11A, O21A and O39, O49, O55, O39A, O49A, O55A), respectively, from two neighboring moieties $[Ni_{0.5}(Mo_6O_{15})(PO_4)(HPO_4)_3]$ and $[Ni_{0.5}(Mo_6O_{15})(PO_4)(H_2PO_4)_2(HPO_4)]$. Ni2 is coordinated with four oxygens (O29, O31, O34, and O35) of four P–O groups (P1, P4, P5, and P6) from two different $[P_4Mo_6]$ units and two terminal coordinated waters. Ni3, Ni4, and Ni6 exhibit octahedral NiN_4O_2 coordination. Ni3 is bonded with an oxygen (O62) from a P–O group (P8), four nitrogens from two bpy ligands, and a coordinated water. Ni4 is bonded with an oxygen (O64) from a P–O group (P7), four nitrogens from two bpy ligands, and a coordinated water. Ni3 and Ni4 link two P–O groups of the $Ni5_{0.5}[P_4Mo_6]$ unit (figure S1). Ni6 coordinates to four nitrogens from two bpy ligands and two coordinated waters. Bond-valence calculations [26] indicate that all the Mo, Ni, and P centers display the +5, +2, and +5 oxidation states. Furthermore, the μ_2-O between nonbonding Mo atoms (O2, O8, O16 and O42, O45, O52) and part of P–O groups (O25, O26, O27, O28, O30, O59, O61, and O63) are protonated. These results are consistent with charge balance considerations.

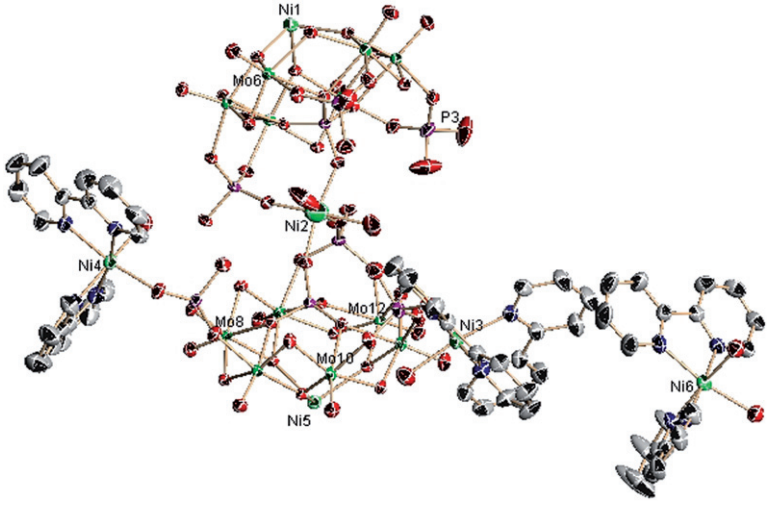

Figure 1. ORTEP drawing of **1** with thermal ellipsoids at 50% probability.

As shown in figure 2, Ni1$[P_4Mo_6]_2$ and {Ni5$[P_4Mo_6]_2$[Ni$(bpy)_2(H_2O)]_4$} are alternately connected by [Ni$(H_2O)_2$] subunits, forming an unusual 1-D chain. The [Ni$(bpy)_2(H_2O)$] complex cations and free water molecules are located at the space of adjacent chains. The adjacent chains are packed together and exhibit 3-D supermolecular structure *via* extensive hydrogen-bonding interactions between bpy groups and polyoxoanions (figure 3).

3.3. *IR and UV-Vis spectra*

In the IR spectrum of **1** (figure S2), characteristic peaks at 968, 747, 691, 550, and 1039 cm^{-1} are assignable to the ν(Mo=O), ν(Mo–O–Mo), and ν(P–O) stretches. A series of medium intensity bands at 1078–1639 cm^{-1} is associated with 2,2′-bpy, and a broad and strong band at 3423 cm^{-1} is associated to water.

The UV-Vis spectrum of **1** displays intense absorption at 203 nm, assigned to $O_t \rightarrow$ Mo charge-transfer (figure S3). Two absorptions at 227 and 252 nm are assigned to $O_{b,c} \rightarrow$ Mo charge-transfer. A shoulder at 281 nm is due to adsorption of 2,2′-bpy ligands.

3.4. *TG analyses*

Compound **1** has three steps of weight loss, as shown in figure S4. The first is 6.15% in the temperature range of 160–220°C, corresponding to the loss of crystal water (Calcd 6.31%). The second is 2.38% from 220°C to 330°C, corresponding to the loss of coordinated water (Calcd 2.71%). The third is 24.31% from 370°C to 600°C, corresponding to the loss of 2,2′-bpy (Calcd 23.44%). The whole weight loss is 32.84%, which is in agreement with the calculated value (32.46%). The TG curve of **1** supports its chemical composition.

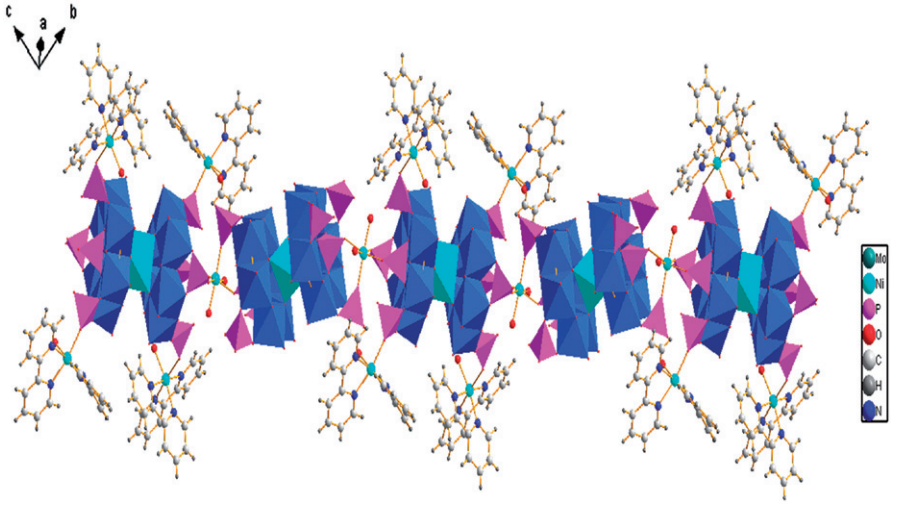

Figure 2. Polyhedral and ball-stick representation of the 1-D chain in **1**.

3.5. *Fluorescent analyses*

The emission spectrum of **1** in the solid state at room temperature is depicted in figure 4. Compound **1** exhibits photoluminescence with an emission maximum at 548 nm upon excitation at 388 nm. Free 2,2′-bpy displays a weak luminescence at 530 nm in the solid state at room temperature. Wang *et al.* [25] reported that $[Cd_4(2,2'\text{-bpy})_2(H_2O)_4][Cd(2,2'\text{-bpy})(H_2O)]_2[Cd(HPO_4)_4(HPO_4)_4(MoO_2)_{12}(OH)_6]\cdot 3H_2O$ exhibits photoluminescence with an emission maximum at 431 nm upon excitation at 400 nm. Hong *et al.* [27] reported that $[Zn_2(2,2'\text{-bpy})_2(ip)_2]_n$ exhibits intense photoluminescence at 439.9 nm upon photoexcitation at 380 nm. Chen *et al.* [28] reported that $[Cd_2(mpa)_2(2,2'\text{-bpy})_2]_n$

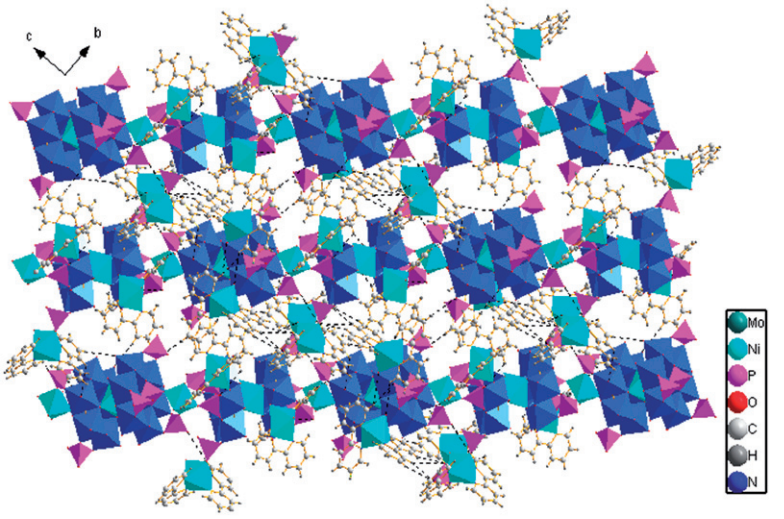

Figure 3. Polyhedral and ball-stick representation of the 3-D supramolecular network by hydrogen bonds in **1**.

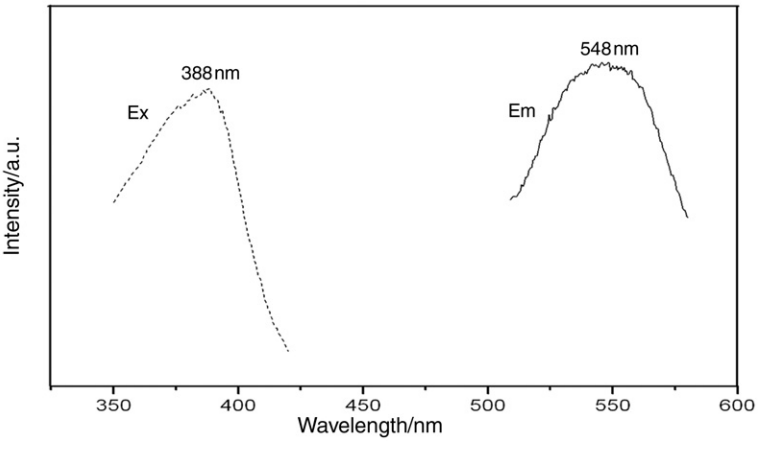

Figure 4. The excitation spectrum and emission spectrum of **1** in the solid state at room temperature.

exhibits two intense emission maxima at *ca* 405 and 422 nm upon excitation at *ca* 347 and 355 nm, respectively. According to these reports, the emission band could be assigned to the ligand-to-metal charge transfer (LMCT) emission. The red-shift may be attributed to the enlargement of conjugation after coordination and thus the lowering of emission state level of the ligand. Since hydrothermal products are usually stable, it is possible to develop high-stable luminescent materials based on **1**.

3.6. *Voltammetric behavior of 1-CPE in aqueous electrolyte*

Electrochemical studies of a **1**-CPE were carried out in 1 M H_2SO_4 aqueous solution. Figure 5 shows the cyclic voltammogram of **1**-CPE in 1 M H_2SO_4. Three redox couples were observed in the potential domain of +500 to −600 mV. The mean peak potentials $E_{1/2} = (E_{pa} + E_{pc})/2$ were +216 mV (I), +50 mV (II), and −246 mV (III) (scan rate: 20 mV s^{-1}), respectively. E_{pc} and E_{pa} are cathodic and anodic peak potentials. Redox peaks I/I′, II/II′, and III/III′ are ascribed to three consecutive redox processes of Mo [29]. The peak potential separations of these three pairs of redox peaks are 130, 103, and 298 mV; these values deviate from zero, the value expected for a reversible surface redox process, perhaps because of the nonideal behavior [30]. With the scan rate varying from 10 to 80 mV s^{-1} (figure S5), the peak currents are proportional to the scan rate, which indicates that the redox process is surface controlled [31]. The peak potentials of three pairs of redox peaks change gradually: the cathodic peak potentials shift toward the negative directions and the corresponding anodic peak potentials to the positive direction. The peak-to-peak separation between the corresponding cathodic and anodic peaks increases with the scan rate increasing. The potential shifts of the three redox peaks in **1**-CPE may relate to the effect of polyanions and the organic–inorganic hybrid framework.

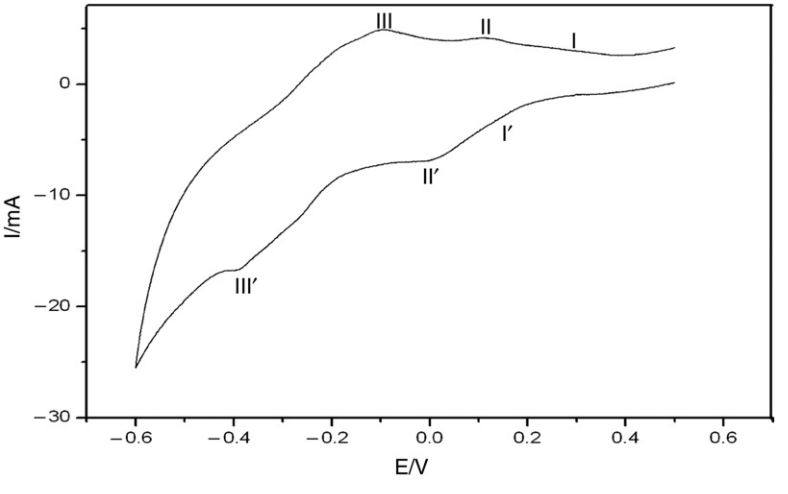

Figure 5. The cyclic voltammogram of **1**-CPE in 1 M H_2SO_4 solution. Scan rate: 20 mV s^{-1}.

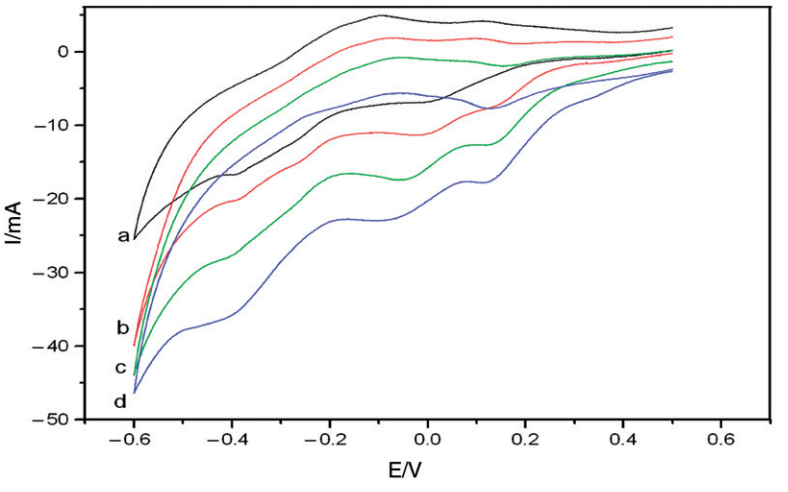

Figure 6. The cyclic voltammograms of **1**-CPE in 1 M H_2SO_4 containing (a) 0; (b) 3; (c) 7; and (d) 10 mM $NaBrO_3$. Scan rate: 20 mV s^{-1}.

3.7. *Electrocatalytic reduction of bromate on 1-CPE*

The electrocatalytic reduction of bromate in 1M H_2SO_4 was investigated at **1**-CPE (figure 6). Our studies indicate that **1**-CPE has good electrocatalytic activity toward the reduction of bromate. With the addition of bromate, the peak-to-peak separations between the corresponding anodic and cathodic peaks increased, all reduction peak currents at negative domain increase remarkably, while all corresponding oxidation peak currents decrease, suggesting that reduction of bromate is mediated by reduced $[P_4Mo_6]$ clusters in **1**.

4. Conclusion

We report a new 1-D chain "heteropoly blue" based on $[P_4Mo_6]$ clusters and nickel complexes. The synthesis of **1** indicates that $[P_4Mo_6]$ is a versatile building block and shows the perspective of extending the POMs family through reasonably choosing the POMs clusters and selecting suitable second metals and organic ligands. Based on this work, further investigations of high-dimensional "heteropoly blues" consisting of $[P_4Mo_6]$ clusters and TMCs are under way in our laboratory.

Supplementary material

The IR, UV-Vis, and TG of **1** are available. Crystallographic data for the structural analysis reported in this article have been deposited with the Cambridge Crystallographic Data Centre with the deposited CCDC No. 720034. The data can

be obtained, free of charge, from the CCDC, 12 Union Road, Cambridge CB2 1EZ, UK *via* Fax: +44-1223-336033 or Email: deposit@ccdc.cam.ac.uk.

Acknowledgments

This work is supported by the National Natural Science Foundation of China (20971032), the Study Technological Innovation Project Special Foundation of Harbin (RC2009XK018008).

References

[1] A. Müller, F. Reters, M.T. Pope, D. Gatteschi. *Chem. Rev.*, **98**, 239 (1998).
[2] J. Salta, Q. Chen, Y.D. Chang, J. Zubieta. *Angew. Chem. Int. Ed. Engl.*, **33**, 757 (1994).
[3] X.K. Fang, T.M. Anderson, W.A. Neiwert, C.L. Hill. *Inorg. Chem.*, **42**, 8600 (2003).
[4] H.L. Chen, Y. Ding, X.X. Xu, E.B. Wang, W.L. Chen, S. Chang, X.L. Wang. *J. Coord. Chem.*, **62**, 347 (2009).
[5] X.J. Wang, X.M. Lu, P.Z. Li, X.H. Pei, C.H. Ye. *J. Coord. Chem.*, **61**, 3753 (2008).
[6] M.L. Wei, H.Y. Xu, R.P. Sun. *J. Coord. Chem.*, **62**, 1989 (2009).
[7] J.P. Wang, D. Yang, J.Y. Niu. *J. Coord. Chem.*, **61**, 3651 (2008).
[8] R.C. Haushalter, L.A. Mundi. *Chem. Mater.*, **4**, 31 (1992).
[9] C. du Peloux, A. Dolbecq, P. Mialane, J. Marrot, E. Rivière, F. Sécheresse. *Angew. Chem. Int. Ed. Engl.*, **40**, 2455 (2001).
[10] R.C. Haushalter, F.W. Lai. *Inorg. Chem.*, **28**, 2904 (1989).
[11] S.T. Zheng, J. Zhang, G.Y. Yang. *Inorg. Chem.*, **44**, 2426 (2005).
[12] M.I. Khan, E. Yohannes, R.J. Doedens. *Inorg. Chem.*, **42**, 3125 (2003).
[13] Y. Lu, Y. Xu, E.B. Wang, J. Lü, C.W. Hu, L. Xu. *Cryst. Growth Des.*, **5**, 257 (2005).
[14] Y.S. Zhou, L.J. Zhang, H.K. Fun, J.L. Zuo, I.A. Razak, S. Chantrapromma, X.Z. You. *New J. Chem.*, **25**, 1342 (2001).
[15] Y.S. Zhou, L.J. Zhang, X.Z. You, S. Natarajan. *Inorg. Chem. Commun.*, **4**, 299 (2001).
[16] L.A. Mundi, R.C. Haushalter. *Inorg. Chem.*, **31**, 3050 (1992).
[17] C. Streb, D.L. Long, L. Cronin. *CrystEngComm.*, **8**, 629 (2006).
[18] H.X. Guo, S.X. Liu. *Inorg. Chem. Commun.*, **7**, 1217 (2004).
[19] X. Zhang, J.Q. Xu, J.H. Yu, J. Lu, Y. Xu, Y. Chen, T.G. Wang, X.Y. Yu, Q.F. Yang, Qi. Hou. *J. Solid State Chem.*, **180**, 1949 (2007).
[20] Z.F. Zhao, B.B. Zhou, Z.H. Su, X. Zhang, G.H. Li. *Cryst. Growth Des.*, **6**, 632 (2006).
[21] Z.F. Zhao, B.B. Zhou, Z.H. Su, H.Y. Ma, C.X. Li. *Inorg. Chem. Commun.*, **11**, 648 (2008).
[22] Z.H. Su, B.B. Zhou, Z.F. Zhao, X. Zhang. *Inorg. Chem. Commun.*, **11**, 334 (2008).
[23] G.M. Sheldrick. *SHELXS-97, Program for X-ray Crystal Structure Solution*, University of Göttingen, Göttingen, Germany (1997).
[24] G.M. Sheldrick. *SHELXL-97, Program for X-ray Crystal Structure Refinement*, University of Göttingen, Göttingen, Germany (1997).
[25] Y. Ma, Y.G. Li, E.B. Wang, Y. Lu, X.L. Wang, X.X. Xu. *J. Solid State Chem.*, **179**, 2367 (2006).
[26] N.E. Brese, M. O'Keeffe. *Acta Crystallogr.*, **B47**, 192 (1991).
[27] Y.F. Zhou, Y.J. Zhao, D.F. Sun, J.B. Weng, R. Cao, M.C. Hong. *Polyhedron*, **22**, 1231 (2003).
[28] L.Y. Zhang, G.F. Liu, S.L. Zheng, B.H. Ye, X.M. Zhang, X.M. Chen. *Eur. J. Inorg. Chem.*, 2965 (2003).
[29] K. Unoura, N. Tanaka. *Inorg. Chem.*, **22**, 2963 (1983).
[30] H. Fu, W.L. Chen, E.B. Wang, J. Liu, S. Chang. *Inorg. Chim. Acta*, **362**, 1412 (2009).
[31] Z.G. Han, Y.L. Zhao, P. Jun, Y.H. Feng, J.N. Yin, Q. Liu. *Electroanalysis*, **17**, 1097 (2002).